

Low-Frequency Noise Characteristics of GaAs Schottky Diodes Fabricated by In-Situ Electrochemical Process and comparison to Evaporation Process

P. Marsh, D. Pavlidis, and M. Tutt,

Dept. of EECS
The University of Michigan,
Ann Arbor MI. 48109-2122

T. Hashizume

Hokkaido Polytechnic College,
Zenibako 3-190,
Otaru 047-02, Japan

H. Hasegawa and T. Sawada

Research Center for Interface Quantum Electronics
Hokkaido University
Sapporo 060, Japan

A. Grüb and H.J. Hartnagel

Institut für Hochfrequenztechnik
Technische Hochschule Darmstadt
W-6100 Darmstadt, Germany

Abstract

GaAs Schottky diodes grown by MBE have been characterized by DLTS and low-frequency noise techniques. DLTS characteristics of diodes with conventional E-beam evaporated-metal anodes revealed three process-induced trap levels, S_1 , S_2 , and S_3 ; with activation energies of 0.08, 0.27, and 0.55eV respectively. Electrochemically processed diodes showed an absence of S_1 , S_2 traps. The S_1 - S_3 trap densities were significant to only a depth of 1000Å. A study of the signature plots showed the similarity of these defects to those produced by irradiation. Low-frequency noise spectra were studied as functions of dc current and temperature over the frequency range of 10Hz to 10MHz. In both types of diodes noise current fell with temperature and increased with dc current. Measurements at 300K and 10mA indicated that the electrochemically processed diodes had significantly lower generation-recombination current and lower noise above 6KHz than those processed by E-beam.

I. Introduction

Currently, the lack of low-noise amplifiers at submillimeter and THz frequencies means that the mixer is the first component seen by the incoming signal. Therefore, the mixer's equivalent input noise temperature sets the lower limit of a receiver's noise.

GaAs Schottky diodes are a key element in heterodyne mm and sub-mm wave receivers. Techniques for the realization of their Schottky contacts include evaporation of Pt or Ti by electron-beam and in-situ anodic pulse etching followed by electrochemical Pt deposition [1]-[3]. Noise characteristics are a key factor in successful use of Schottky diodes in sub-mm wave receivers. Since traps can play a significant role in the noise performance of Schottky diodes, it is consequently very important to evaluate process techniques that show potential for reduction of trap densities and consequently, noise. This paper addresses such issues for diodes prepared by the novel in-situ electrochemical etching/plating process and conventional E-beam evaporation techniques.

Traps have often been correlated to bulk defects and interface states at the Schottky-semiconductor boundary. Low concentrations of these traps are usually accompanied by good ideality factors, small reverse-bias leakage, low recombination currents and most importantly, lower noise temperatures in mixers. This provides a motivation for the

implementation of fabrication techniques which reduce these trap concentrations. Using Deep Level Transient Spectroscopy (DLTS) characterization, it was shown that a novel electrochemical anodic etch followed by in-situ Pt plating technique (hereafter referred to as electrochemical etch/plating) resulted in the virtual elimination of two of three traps normally found in anodes fabricated via E-beam metal evaporation (hereafter referred to as evaporation). The electrochemically etched/plated anodes also tended to exhibit superior ideality factors compared to those of the E-beam anodes. Since the electrochemical etch/plating technique appears to result in overall improved diode characteristics, it is of considerable interest to study whether it can improve noise performance as well. The purpose of this paper is to compare the low-frequency noise performance of diodes fabricated by E-beam evaporated metal (hereafter referred to as evaporated diodes) against those fabricated via in-situ electrochemical etch/plating (hereafter referred to as plated diodes).

In section II, the trap characteristics of evaporated and plated diodes are compared by DLTS. Section III compares the I-V and low-frequency noise properties of evaporated and plated diodes. Finally, conclusions are discussed in section IV.

II. DLTS Study of Diodes

II-A. Device Structure and Fabrication

All diodes characterized here via DLTS were fabricated on the same n+ GaAs wafer having a $0.2\mu\text{m}$ GaAs epilayer grown by molecular beam epitaxy (MBE) and doped with Si at $n = 2 \times 10^{16}/\text{cm}^3$. Both evaporated and plated Schottky's were formed from Pt covered by Au and then passivated with SiO_2 . The evaporated diodes' anodes were formed via conventional E-beam evaporation of Pt while plated diodes were formed using the new electrochemical etch/plating process illustrated below in Fig 1.

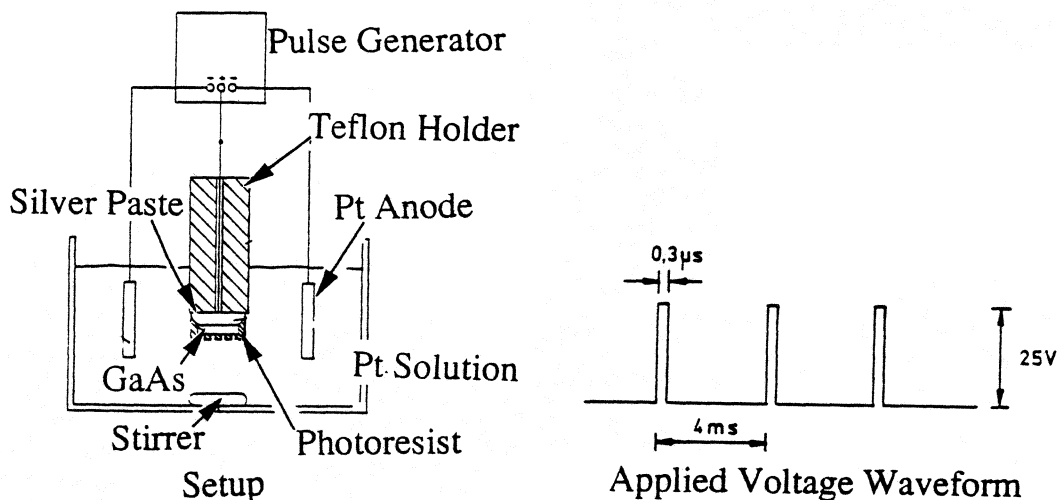


Figure 1. Pulse anodic etch followed by in-situ platinum plating process technique.

In the electrochemical etch/plating process, the Pt plating solution serves both to etch the semiconductor and form the electroplated anodes. First, the anode regions are etched to expose a high-quality semiconductor surface. Etching is accomplished by pulsing the semiconductor positive while it is in the acid Pt plating solution. While the

semiconductor is positive, holes appearing at the solution-semiconductor interface oxidize the semiconductor surface. During the relatively long intervals between pulses, oxidation stops and reaction products dissipate, allowing anisotropic etching [4]. The low pH of the etching solution acts to remove oxides. In this work, the etch rate was 40Å/pulse. Immediately after etching, the semiconductor is pulsed negative to plate Pt onto the anode regions. It is believed that this in-situ process achieves superior Schottky contacts by reducing the amount of oxides and other contaminants under the Schottky metal.

II-B. I-V Results

Fig. 2 illustrates evaporated and plated I-V curves. I-V curves of the evaporated diodes showed barrier heights (ϕ_b) in the range 0.80-0.85eV [1]. Plated diodes had higher ϕ_b 's in the range of 0.95-1.00eV. Plated diodes exhibited ideality factors (η) ≤ 1.05 , while evaporated diodes had $\eta > 1.1$.

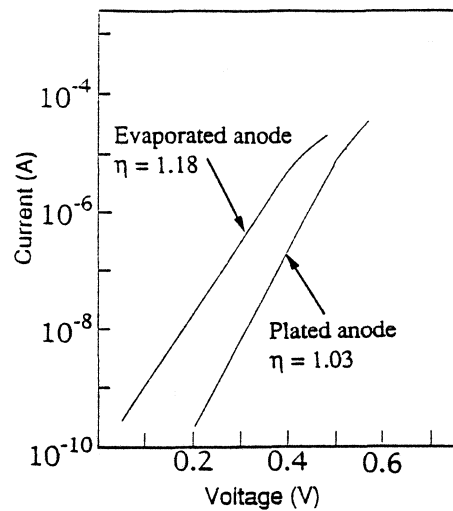


Figure 2. Evaporated and plated diode I-V curves.

II-C. DLTS Analysis

DLTS measurements showed the appearance of several traps not normally found in native bulk GaAs [1]. These traps are thought to be process-induced because they do not appear in bulk MBE GaAs and their concentrations are significant to a depth of only about 1000Å (Fig. 3). The evaporated diodes exhibited the process-induced traps S_1 , S_2 , and S_3 while the plated diodes exhibited only one such trap, S_3' , having properties very close to those of S_3 . Activation energies (E_a) of S_1 , S_2 , and S_3 were 0.08, 0.27, and 0.55eV, respectively. Fig. 3 indicates that in 200 μ m anodes, the concentration of S_3' was higher than that of S_3 . However, when the anode diameter is reduced to 15 μ m, the situation is reversed, i.e. the DLTS signal of S_3' is now less than that of S_3 . Thus, at a depth of 500Å, the 15 μ m plated diode has a total trap concentration of $\leq 2.7 \times 10^{14}/\text{cm}^3$ vs. $4.7 \times 10^{14}/\text{cm}^3$ for the evaporated diode. The dependence of S_3' on anode size is believed to be the result of optimizing the electrochemical etch/plating for the 15 μ m diodes, inadvertently resulting in suboptimal processing of the larger diodes. Recently, it has been determined that reduction of the etch rate in the electrochemical etch/plating process resulted in reduced levels of S_3' in 500 μ m diameter diodes [5].

The signature plots of S_1 - S_3 traps are very similar to those of traps in GaAs arising from irradiation by γ rays and high-energy (1 MeV) electrons [1]. Furthermore, low-energy (≈ 3 KeV) electrons produce traps having signature plots similar to those of the MeV electrons [1]. Since irradiation by low-energy stray electrons is likely during the E-beam metal evaporation-deposition process, the traps S_1 - S_3 are thought to be the result of defects formed by the stray electrons during this process.

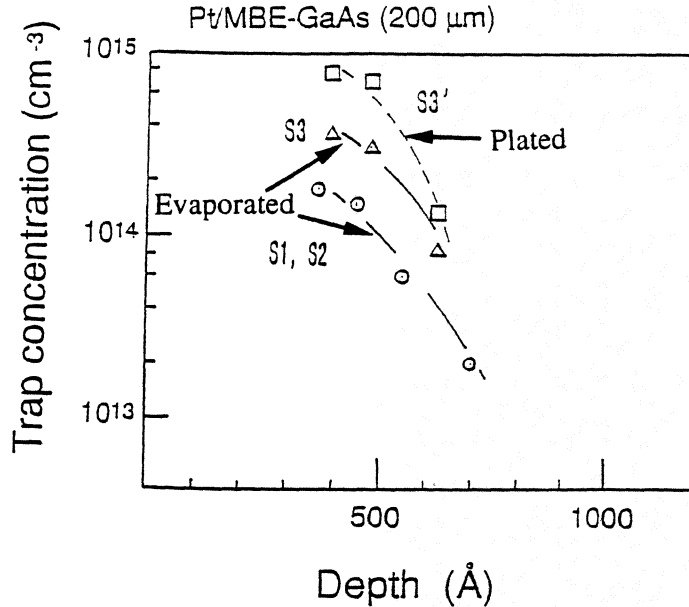


Figure 3. Trap concentrations vs. depth.

III. Low-Frequency Noise Characterization

III-A. Theory of Trap Noise

The spectral characteristic of the mean noise current squared, $S_I(f)$, from an ensemble of identical traps typically exhibits a Lorentzian behavior having the form [6]:

$$S_I(f) = \frac{C_2 \tau F_t (1 - F_t)}{1 + (\omega \tau)^2} \quad (\text{A}^2/\text{Hz}) \quad (1)$$

Where:

- $V_b = q\phi_b$
- $C_2 = \text{constant.}$
- $\tau = \text{characteristics trap time constant.}$
- $F_t = \text{occupation probability of the trap.}$
- $\omega = \text{the radian frequency.}$

For electron traps [6], at low current densities the characteristic time, τ follows:

$$\tau \propto \exp\left(\frac{E_a}{KT}\right) \quad (2)$$

Where: E_a = trap activation energy
 K = Boltzmann's constant,
 T = temperature in Kelvin.

Also, it is possible to define a characteristic trap frequency $f_{tr} = \frac{1}{2\pi\tau}$.

Since the quantity $F_t(1-F_t)$ is a maximum at $F_t = 0.5$ i.e. the only traps that will contribute significantly to the noise are those that lie near the local Fermi level, i.e. are statistically half occupied. For the case where traps are distributed uniformly in E_a and space, the resulting continuum of time constants has the proper distribution to give $S_I(f)$ a $1/f$ form over a region of frequencies [7]. At a sufficiently low frequency, $S_I(f)$ will plateau. In the $1/f$ range, $S_I(f)$ will be proportional to the anode current squared (I_d^2) [7]. At very low frequencies where $S_I(f)$ becomes constant, $S_I(f)$ is proportional to $I_d^{1.5}$ [7].

III-B. Device Structure and Fabrication

The evaporated and plated diodes characterized for low-frequency noise have the same cross-section and epilayer doping as the diodes discussed in section II, except that the epilayer is $0.9\mu\text{m}$. All characterized devices had anode diameters of $50\mu\text{m}$ and were from the same MBE GaAs wafer.

Prior to anode deposition, the evaporated diodes' anode areas were etched using $\text{NH}_4\text{OH}/\text{H}_2\text{O}_2/\text{H}_2\text{O}$ in a (2:1:300) ratio. Next, E-beam evaporated metals in the sequence Ti/Pt/Au were deposited. Finally, Au was plated onto the anodes to facilitate wirebonding and probing.

The plated diodes' anodes were anodically etched then plated in-situ with Pt as discussed in section II-A. The plated Pt anodes were then completed with an Au deposition over the Pt.

III-C. Measurements Performed

Several diodes from both the plated anode and evaporated anode samples were subjected to the following comparative tests:

1. I-V characteristics vs. temperature.
2. $S_I(f)$ vs. I_d , $10\text{Hz} \leq f \leq 10\text{MHz}$, at room temperature ($\approx 300\text{K}$).
3. $S_I(f)$ ($10\text{Hz} \leq f \leq 10\text{MHz}$) vs. temperature ($125\text{K} - 300\text{K}$) with $I_d = 10\text{mA}$.

III-D. Measurement Setup and Procedure

Both the evaporated and plated samples were mounted on gold metallized alumina coplanar chip carriers designed for a coplanar waveguide microwave test fixture. Diodes were wirebonded to the chip carrier transmission lines to eliminate vibration-induced contacting noise. Room temperature testing was performed with the chip carrier mounted into the microwave test fixture, whereas variable-temperature measurements were performed in a cold stage. The measurement setup is shown below in Fig. 4 below.

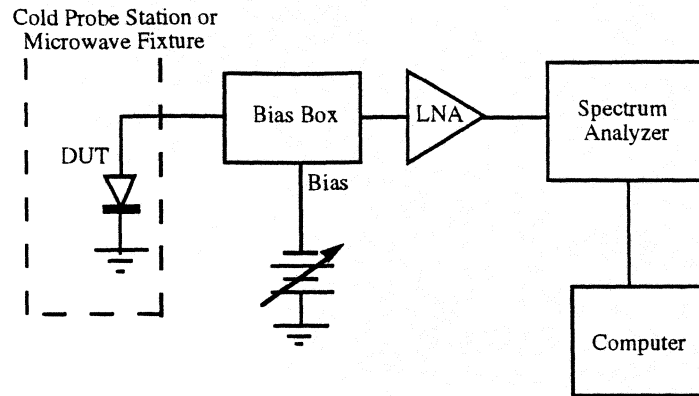


Figure 4. Measurement test setup for low-frequency noise characterization of diodes.

At measurement frequencies below 100KHz, the spectrum analyzer was an HP 3561A dynamic signal analyzer. The 100KHz to 10MHz frequency range was covered by a Tektronix 2755P spectrum analyzer.

$S_I(f)$ (A^2/Hz) is derived from $V_{mn}(f)(V/\sqrt{Hz})$, the RMS noise voltage at the diode terminals, via the use of a diode noise model. The diode model consists of R_{ohm} in series with the parallel combination of R_i , and the noise current source, $I_n(f)$ (A/\sqrt{Hz}). R_{ohm} is the portion of the diode resistance due to ohmic resistance from the conductive mounting paint, n+ GaAs substrate, and finally the undepleted portion of the n- epilayer. R_i is due to the dynamic resistance of the Schottky barrier itself. The total resistance presented to the diode by the bias box and LNA during the noise tests is represented by R_L . $V_{mn}(f)$, is extracted by subtracting the noise floor power from the raw spectrum analyzer reading, then referring the result to the LNA input. Next, $I_n(f)$ is extracted from $V_{mn}(f)$ using the diode noise model. Finally, $S_I(f)$ is derived from:

$$S_I(f) = \langle |I_n(f)|^2 \rangle \quad (3)$$

This model assumes that all diode noise mechanisms originate entirely within the depletion region. This is believed to be accurate for the analysis here since electron traps should be mostly inactive within the undepleted GaAs as they will be always filled. Also, the low current densities used here should not cause significant additional noise due to hot electrons.

Extraction of the diode model's resistances, R_i , and R_{ohm} , make use of the diode relation:

$$\log(R_i) = m \cdot \log(I_d) + b \quad m \text{ and } b \text{ are constants} \quad (4)$$

Due to nonzero R_{ohm} and other effects, the relation (4) is accurate only over a limited range of I_d . Here, (4) was found to be quite accurate for $I_d = 100\mu A$. Also at $I_d = 100\mu A$ $R_i \approx \frac{\Delta V_d}{\Delta I_d}$. To find $R_i |_{I_d'}$, (R_i at the diode current I_d'):

$$R_i |_{I_d'} = \left(\frac{100\mu A}{I_d'} \right) \left(\frac{\Delta V_d}{\Delta I_d} |_{I_d = 100\mu A} \right) \quad (5)$$

And:

$$R_{ohm} I_{d'} = \frac{\Delta V_d}{\Delta I_d} I_{d'} - R_i I_{d'} \quad (6)$$

III-E. I-V Results

I-V characteristics of several evaporated and plated diodes were plotted in Fig. 5. The in-situ anode plating process yields higher barrier potentials (ϕ_b) and lower generation-recombination current than the evaporated anode process. At $I_d = 10\text{mA}$ and 300K , R_i and R_{ohm} for the evaporated and plated diodes are nominally 2.4Ω and 1.4Ω respectively. At 300K ideality factors (η) of the evaporated and plated diodes have nominal values of 1.19 and 1.14, respectively. As temperatures fall, tunneling becomes more significant resulting in the evaporated diode's η rising to 1.54 at 125K . Similarly, the plated diode's η rose to 1.50 at 125K . Barrier height was calculated via:

$$\gamma \equiv \ln\left(\frac{I_d}{T^2}\right) - \frac{V_d}{\eta K T} = \ln(A_e A^*) - \left(\frac{V_b}{K}\right) \frac{1}{T} \quad (7)$$

where: $V_b = q\phi_b$

A_e = effective anode area,

A^* = effective Richardson's constant and

V_d = applied diode voltage.

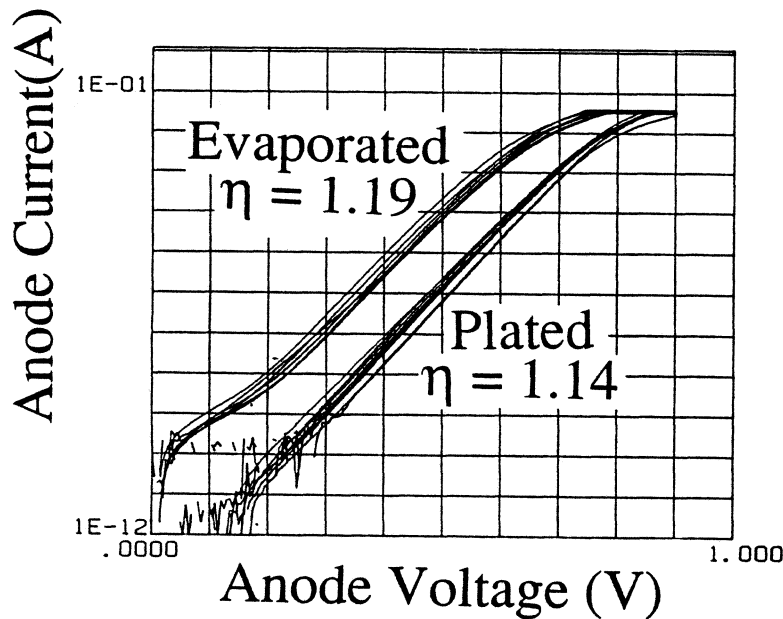


Figure 5. IV curves of several plated and evaporated diodes.

Barrier heights (ϕ_b) were obtained from the slope of a least-squares linear fit of γ vs. $\frac{1}{T}$ over 225K to 300K . At low temperatures γ deviates upward from the linear fit because of rising η . One of the evaporated diodes (Ti) had $\phi_b = 0.651\text{eV}$ vs. $\phi_b = 0.832\text{eV}$ for a

plated (Pt) diode. In comparison, Ti and Pt Schottky's on GaAs are reported to have measured ϕ_b 's of 0.82eV and 0.86eV respectively [8].

III-F. Low-Frequency Noise Results

1. Noise vs. I_d @ 300K

Figs. 6 and 7. illustrate 10Hz-10MHz noise spectra vs. I_d for an evaporated diode and a plated diode. Noise was characterized at 300K and $I_d = 0.316, 1.0, 3.16, 10.0,$ and 31.6mA .

Noise spectra for the evaporated diode follow a $1/f$ dependence up to about 100Hz. Above 100Hz the frequency dependence is reduced and then increases again past about 100kHz. This plateau followed by the rapid rolloff is indicative of a group of traps having f_{tr} 's ranging from $\approx 10\text{kHz} - 10\text{MHz}$.

In contrast, the plated diode's $1/f$ range extends to roughly 1kHz. Also beyond 100kHz, the plated diode's noise tends to roll off faster than that of the evaporated diode's, pointing to a more ideal $1/f$ behavior. Above 1MHz and at $I_d = 0.316\text{mA}$, both diodes' noise approached the system noise floor. The flat region of $S_I(f > 2\text{MHz})$ at 1mA , for both diodes, is also due to the measurement system noise floor. However, at $I_d = 1\text{mA}$, the shot noise level is $3.2 \times 10^{-22} \text{ A}^2/\text{Hz}$, so that the actual $S_I(f)$ at 1mA would not appear much different than those in Figs. 6 and 7.

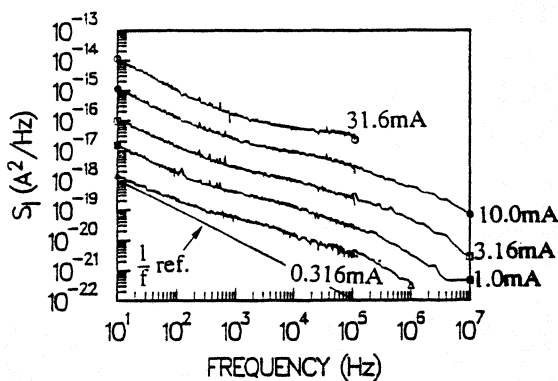


Figure 6. $S_I(f)$ vs. current for an evaporated diode ($T=300\text{k}$).

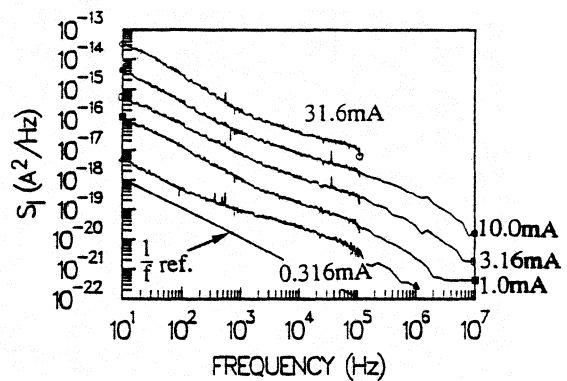


Figure 7. $S_I(f)$ vs. current for a plated diode ($T=300\text{k}$).

In order to draw conclusions about device parameters, several devices per type were measured. Fig. 8 represents the averages of $S_I(f)$ over ensembles of evaporated and plated diodes. At $I_d=10\text{mA}$ and below 6KHz, the evaporated diodes show better noise performance than the plated, while above 6KHz, the reverse is true. Let f_c be defined as the frequency where $S_I(\text{evaporated})=S_I(\text{plated})$. Fig. 9 shows that f_c falls as I_d increases. It is reasonable to presume that f_c largely depends on current density rather than absolute current. Since the diodes tested here are much larger than those that would be actually used in real submillimeter and THz receivers, actual current densities would greatly exceed those used here. Thus with realistic anode sizes, f_c would be considerably lower than shown in Fig. 9, giving plated diodes an even stronger noise performance advantage over evaporated diodes.

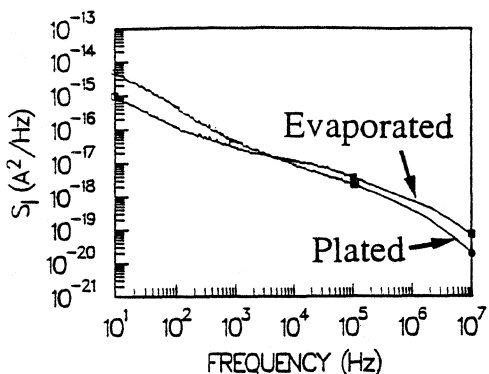


Figure 8. Average of $S_I(f)$ over several diodes of each type ($T = 300K$).

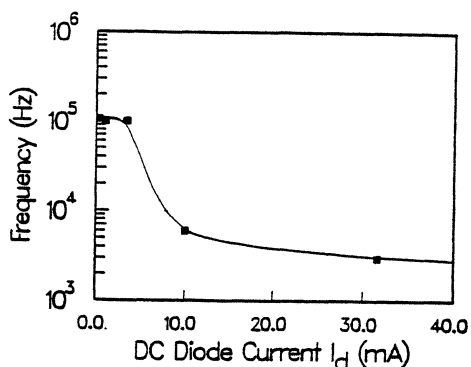


Figure 9. Crossover point (f_c) vs. I_D ($T=300k$).

In Fig. 10, $S_I(f)$ is plotted as a function of I_D for the plated diodes. The plated diode shows the corresponding dependency: $S_I(10Hz) \propto I_D^{1.81}$. Similarly, the evaporated diode's current dependency is: $S_I(10Hz) \propto I_D^{1.92}$. These results agree well with [7] where, for an ensemble of traps distributed uniformly in energy and space throughout the depletion region, $S_I(f) \propto I_D^{2.0}$.

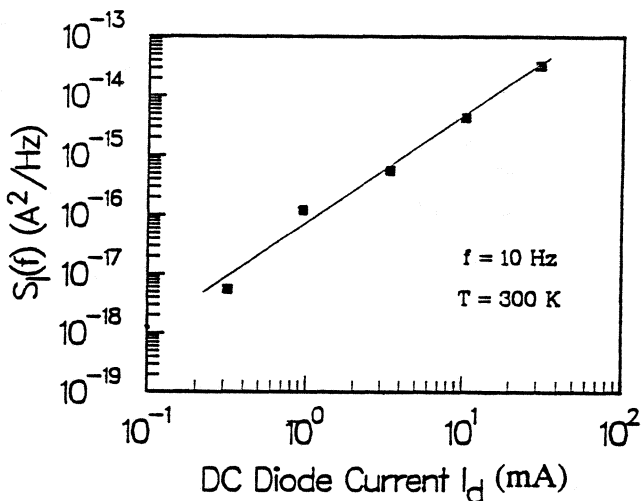


Figure 10 Plated diode noise vs. I_D ($T=300K$).

2. Noise vs. Temperature ($I_D=10mA$)

The evaporated diode's $S_I(f)$ vs. T seems interesting in that there appear to be several characteristic trap frequencies, f_{tr} , which cause a noise bulge for $10KHz < f < 100kHz$. The noise bulge is most likely formed from the traps, giving rise to noise components having Lorentz dependencies. As expected from theory, this noise bulge becomes more prominent and shifts to lower frequencies as the temperature falls. The noise bulge's very slight movement in frequency is indicative of the very small values of activation energies (E_a 's) of the traps causing the bulge. The noise bulge's amplitude is more strongly

affected by temperature than the $1/f$ portion of $S_I(f)$ as would be expected from the theory concerning Lorentz-type $S_I(f)$ functions.

In contrast, as temperature falls, the plated diode's $S_I(f)$ increases in amplitude with very little change in shape. Unlike the evaporated diode, no noise bulges appear in the range 10Hz - 100kHz, thus indicating that the plated diode apparently has no distinct traps with f_{tr} 's between 10Hz-100kHz.

The least-squares linear fit of Fig. 11 shows that $S_I(10\text{Hz}) \propto T^{-2.2}$ and $S_I(10\text{kHz}) \propto T^{-2.9}$ for the evaporated and plated diodes respectively. This is in contrast to theory which predicts $S_I(f) \propto T^{-1.5}$, for regions of $S_I(f)$ having a $1/f$ frequency dependence [7]. The discrepancy of theoretical temperature dependence with respect to that measured may be due to a difference in noise mechanisms for devices here and those postulated in [7]. Also, for evaporated and plated diodes, $S_I(100\text{kHz}) \propto T^{-4.2}$ and $S_I(100\text{kHz}) \propto T^{-2.9}$ respectively (fig. 11). The evaporated diode's increase of temperature dependency at 100kHz reflects the effects of the Lorentz-like noise hump discussed earlier.

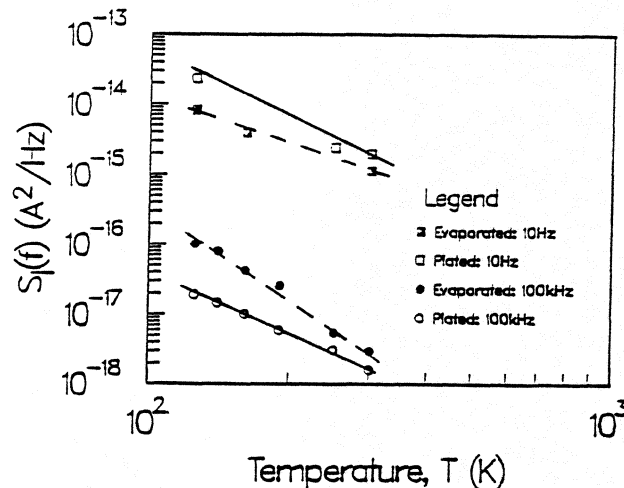


Figure 11. Noise vs. temperature at selected frequencies.

IV. Conclusions

Schottky diodes fabricated using conventional evaporated anodes were compared with those fabricated using a novel anodic and plating technique. DLTS characterization shows that plated diodes have only one process-induced trap whereas evaporated diodes show three such traps. These traps are only significant to a depth of 1000\AA and are similar to those induced by irradiation. Optimized plated diodes also show lower overall trap densities. For example, at 500\AA depth, an optimized plated diode yielded process-induced trap concentrations of $\leq 2.7 \times 10^{14}/\text{cm}^3$, vs. $4.7 \times 10^{14}/\text{cm}^3$ for the evaporated-anode process. In contrast to the evaporated diodes, plated diodes show no detectable generation-recombination current, an $\eta(\text{plated})$ of 1.14 vs. $\eta(\text{evaporated})$ of 1.19, and a $\phi_b(\text{plated})$ of 0.83eV vs. $\phi_b(\text{evaporated})$ of 0.65eV. At $I_d = 10\text{mA}$ and 300K, $S_I(10\text{MHz})$ of the plated diode is lower than that of the evaporated diode and $S_I(\text{plated})$ remains

lower than S_1 (evaporated) for $f > f_c = 6\text{KHz}$. Since f_c falls with current density, actual THz diodes are expected to have an f_c considerably below the 6KHz for the large diodes measured here. Temperature dependent measurements revealed the presence of shallow traps in evaporated diodes not observed in plated diodes. In conclusion, the work presented here shows that the new in-situ plating process has significantly improved junction quality and noise performance over diodes fabricated using the more-conventional E-beam evaporated metal process. The advantage of the in-situ etch-plating process is expected to increase as this process becomes better understood and optimized.

References

- [1] T. Hashizume, H. Hasegawa, T. Sawada, A. Grüb and H.L Hartnagel, "Deep Level Characterization of Submillimeter-Wave GaAs Schottky Diodes Produced by a Novel In-Situ Electrochemical Process", Japanese Journal of Applied Physics Vol. 32 Part 1, No. 1B, Jan. 1993 pp. 486-490.
- [2] T. Hashizume, H. Hasegawa, T. Sawada, A. Grüb and H.L Hartnagel, "Deep Level Characterization of Submillimeter-Wave GaAs Schottky Diodes Produced by a Novel In-Situ Electrochemical Process", 1992 Intl. Conf. on SSDM, pp. 257-259.
- [3] A. Grüb, K. Fricke, and H.L. Hartnagel, "Highly Controllable Etching of Epitaxial GaAs Layers by the Pulse Etching Method", J Electrochem. Soc. 138, pp 856-857 (1991).
- [4] A. Jelenski, A. Grüb, V. Krozer, H.L. Hartnagel "A New Approach to the Design of Schottky-Barrier Diodes for THz Mixers" Third International Symposium on Space Terahertz Technology March 24-26 1992, pp 631-642.
- [5] T. Hashizume, Private Communications.
- [6] H.S. Lin, P.A. Colestock, P. Fang, T.M. Chen, "Generation-Recombination Noise in GaAs p-in+ Diodes", IEEE Proceedings - 1989 Southeastcon pp 1295-1297.
- [7] Sheng T. Hsu "Low-Frequency Excess Noise in Metal-Silicon Schottky Barrier Diodes", IEEE Transactions on Electron Devices Vol. ED-15, No. 7 July 1970, pp. 496-506.
- [8] Ralph E. Williams, "Gallium Arsenide Processing Techniques", Artech House Inc., 1984.